


Nanofibrous Membranes for Low-Concentration Cr^{VI} Adsorption: Kinetic, Thermodynamic and the Influence on ZFL Cells Viability

Guilherme Dognani^{a*} , Flávio Camargo Cabrera^{a,b}, Dalita Gomes Silva Morais Cavalcante^a,
Rosane Freire Boina^a, Aldo Eloízo Job^a, Deuber Lincon da Silva Agostini^a

^aUniversidade Estadual Paulista (UNESP), Faculdade de Ciências e Tecnologia (FCT), 19060-080, Presidente Prudente, SP, Brasil.

^bUniversidade Estadual de Maringá (UEM), Departamento de Meio Ambiente, 87506-370, Umuarama, PR, Brasil.

Received: January 06, 2021; Revised: April 07, 2021; Accepted: June 16, 2021

There is a great demand to develop different techniques for the continuous removal, immobilization, and remediation of metallic ions from contaminated water. Human contamination by metallic ions could even occur by ingestion of seafood causing carcinogenic and mutagenic activities. In this study, a nanofibrous membrane of poly (vinylidene fluoride-co-hexafluoropropylene) (PVDF-HFP) produced by electrospinning technique and coated with polyaniline (PAni) was tested for the removal of chromium in low-concentration solutions. The viability of ZFL cells (zebrafish liver cells) was performed to evaluate the water quality enhancement after chromium adsorption. The results indicated that the nanofibrous membrane successfully adsorbed the chromium species in low-concentration ($Q_e = 2.44$ mg/g, at pH 4.5, room temperature (RT) and 24h) by Freundlich model and followed a pseudo-second-order kinetics model indicating a possible chemisorption in multilayers, at pH 4.5, RT and $[Cr^{VI}] = 5.0$ mg/L. At pH 2.0 (24h, RT and $[Cr^{VI}] = 5.0$ mg/L), the membrane adsorbed around 91.64% of Cr^{VI} contaminants. The thermodynamic studies revealed that the process was spontaneous and exothermic. The cells viability demonstrated the efficiency of the membrane tested in the aquatic ecosystem protection; the viability increased 19.2% in 5.0 mg/L Cr^{VI} solution. Thus, the results of this study shows that the nanofibrous membrane can be an alternative to remove low concentration of Cr^{VI} from aqueous solutions.

Keywords: Membrane Technology, Nanofibers, Adsorption, Chromium, Water Decontamination.

1. Introduction

The world progress has brought comfort for people, making the life easy, developing new materials and process, which can be used day by day. With this progress, some disadvantages come together, such as improper waste disposal of solid and liquid materials containing many contaminants^{1,2}. Among the contaminants, metallic ions, such as cadmium³, lead⁴, mercury⁵ and chromium⁶, have been highlighted in several industries like electroplating, batteries, leather tanning, fertilizer and painting industries⁷. In nature, chromium exists in two forms, trivalent and hexavalent chromium. The hexavalent form $[Cr^{VI}]$ is highly toxic and mobile in aqueous solutions, being responsible for environmental contaminations⁸.

Contamination by metallic ions can happen through direct ingestion of contaminated food, consumption of contaminated water, inhalation or even contact with the skin⁹. When in contact with the organism, heavy metals tend to alter the activity or damage proteins, enzymes and DNA molecules, promoting changes which generate diseases as

well as carcinogenic and mutagenic activities^{10,11}. When released into effluents these metals tend to contaminate the aquatic communities, not biologically so they may be bioaccumulated in the food chain since they are found at high concentrations in fish living in contaminated water¹².

Several pathways have been seeking to the removal of chrome pollutants from water by chemical precipitation¹³, electrochemistry reduction¹⁴, reduction by fungi¹⁵, phytoremediation¹⁶, adsorption by cellulose-based materials^{17,18}, adsorption by mesoporous materials^{19,20} and, adsorptive membrane^{7,21,22}.

We have recently introduced the design concept of electrospinning PVDF-HFP/PAni membranes for high concentration of chromium removal from aqueous medium²¹ as well as the good desorption efficiency of these membranes.

Herein, we optimize the use of nanofibrous membrane of PAni-coated electrospun PVDF-HFP nanofibers in low-concentration hexavalent chromium removal from aqueous solutions simulating an industrial effluent released into the environment. In addition, we evaluated the influence of chromium concentration on ZFL cells viability and, the

*e-mail: dognani.g@gmail.com

efficiency of electrospun membranes in the purification of water from chromium.

2. Experimental

2.1. Chemical and materials

Potassium dichromate ($K_2Cr_2O_7$, 99,5%) was acquired from Synth Chemicals, 1,5-Dyphenylcarbazine (ACS-grade) was purchased from Fisher Scientific. Zebrafish (*Danio rerio*) liver cell line (ZFL- BCRJ 0256) was obtained from UFRJ-Brazil, it was supplemented with Leibovitz L-15 medium (Gibco®) and RPMI 1640 medium (Gibco®). All chemicals were used without further purification.

The electrospun membranes used to adsorb the pollutant were produced as described in previous work²¹. Briefly, Poly(vinylidene fluoride-co-hexafluoropropylene) (PVDF-HFP) (Kynar Flex 2821-00®, provided by Arkema Brazil Inc.) was dissolved sequentially in a binary mixture of DMF/acetone at a concentration of 20 wt%. In order to produce membranes, the PVDF-HFP homogeneous solution was electrospun at voltage of 26 kV using the flow rate of 1.0 mL/h and with the tip-collector distance of 15 cm.

2.2. Membrane characterization

The morphology of the electrospun nanofibers was analyzed by Scanning Electron Microscopy (SEM), Carl Zeiss model EVO LS15 using the software ImageJ® as auxiliary. A Mitutoyo 547-526S micrometer was used to study the thickness of the membranes. The contact angle of the membranes was measured using the sessile drop method by a contact angle measuring device OCA15EC using deionized water (DataPhysics, Germany). The porosity of the membrane was defined by gravimetric method, using isopropyl alcohol as a wetting fluid to penetrate the pores of the membrane. The point of zero charge (PZC) of membranes was performed by pH measurement (digital pHmeter AKSD®). The membrane was suspended in 15-mL of water in adjusted pH for 24 h at 25 °C. The pH of each suspension was adjusted to different values ranging from 2 to 11 by adding NaOH and HCl (0.5 and 0.1 M), and the initial and final pH values were recorded^{23,24}. To verify the thermal stability of membrane was carried out Thermogravimetric Analysis (TGA), Netzsch model 209 (10 °C min⁻¹ and N₂ atm).

2.3. Adsorption tests

Potassium dichromate solutions with various Cr^{VI} concentrations ranging from 0.05 to 5.0 mg/L were prepared to study the adsorption capacity of the membranes. In this test, a 10 mg rectangular piece of membrane was immersed into 15 mL of chromium solution at a chosen concentration during 24 h. To analyze the pH effect, solutions with concentrations of 5.0 mg/L and pH values ranging from 2 to 6 were prepared. The contact time test was also carried out with a 5.0 mg/L Cr^{VI} solution at a pH value of 4.2, and time interval from 10 min to 48 h. The Cr^{VI} concentration was determined by a UV-Visible spectrophotometer (Shimadzu, model 1800) using 1,5-diphenylcarbazine (DPC) solution as an indicator at 540 nm²⁵. Briefly, the 10.0 mL of sample was acidified with 0.2 M H₂SO₄ solution (pH ~ 1.0). Then

0.5 mL of freshly prepared 0.25% (w/v) DPC in acetone was added, mixed and let to stand 5 min for full red-violet color development. A calibration curve was created by plotting the absorbance versus known Cr^{VI} concentrations for this test. The amount of Cr^{VI} ions adsorbed on the membrane (mg/g) was calculated by the following equation:

$$Q = \frac{(C_0 - C_f)V}{M} \quad (1)$$

where Q is the amount of Cr^{VI} adsorbed (mg/g), C_0 and C_f are the initial and final Cr^{VI} concentrations (mg/L), respectively, V is the solution volume, and M is the weight of adsorbent membrane used. The adsorption removal rate (R) of Cr^{VI} was also calculated by the equation as follows:

$$R = \frac{(C_0 - C_f)}{C_0} \times 100\% \quad (2)$$

The Langmuir (3) and the Freundlich (4) isotherm models were applied for the mathematical description of the adsorption equilibrium of Cr^{VI} ions on the membrane. The non-linear equations are as follows:

$$q_e = \frac{Q_{max} \cdot k_l \cdot C_e}{1 + k_l \cdot C_e} \quad (3)$$

$$q_e = k_f \cdot C_e^{1/n} \quad (4)$$

where q_e is the adsorption capacity of the membrane at the equilibrium concentration (mg/g), C_e is the equilibrium concentration of metal ion (mg/L), q_m is the maximum adsorption capacity of the membrane (mg/g), b is the Langmuir constant, and k_f is the Freundlich constant²⁶.

To analyze the nature of the kinetics and the rate of Cr^{VI} adsorption, pseudo first-order and pseudo second-order models were used. The non-linear forms of these two models are given in Equations 5 and 6, respectively.

$$q_t = q_e \left(1 - e^{-k_1 t}\right) \quad (5)$$

$$q_t = \frac{k_2 q_e^2 t}{1 + q_e k_2 t} \quad (6)$$

where q_e and q_t denote the amount of Cr^{VI} adsorbed per mass of gram on the membrane surface at equilibrium and at time t , respectively, k_1 and k_2 are the first and second-order rate constants, respectively²⁷.

To conclude if the adsorption is spontaneous or not, the thermodynamic aspects are important. The experimental data obtained at different temperatures (288.15, 298.15, 308.15 and 318.15 K) were used to calculate the thermodynamic parameters such as Gibbs free energy change (ΔG°), enthalpy change (ΔH°) and entropy change (ΔS°). The Gibbs free energy change of the sorption reaction is given by the equations:

$$\Delta G^\circ = -RT \ln k_0 \quad (7)$$

$$K_0 = \frac{C_{Ae}}{C_e} \quad (8)$$

where k_0 is the constant of thermodynamic equilibrium, R is the universal gas constant ($8.314 \text{ J mol}^{-1} \text{ K}^{-1}$), T is absolute temperature (K), C_{Ae} and C_e are the concentration (mg/L) of chromium on the adsorbent and in solution, respectively²⁸.

2.4. MTT assay

The cytotoxic potential of the decontaminated water was evaluated through the *in vitro* MTT assay (3-[4,5-dimethylthiazol-2-yl]-2,5-diphenyl tetrazolium bromide) in different initial concentrations of chromium. ZFL cells were seeded on 10.0 mL of culture medium (50% of Leibovitz L-15, 40% of RPMI, and 10% of fetal bovine serum, with density of 1.2×10^5 cells well plate). The cells were incubated for 24 h with culture (CTR). A positive control using Triton X 1% was also prepared. It was kept in a free-CO₂ incubator at 28 °C.

Then, the culture medium was removed and dimethyl sulfoxide (DMSO) was added and the absorbance corresponding to each sample was determined at 540 nm. The absorbance obtained for the CTR cells was considered as 100% of cell viability, which was determined by Equation 9²⁹:

$$CVK = \frac{AK - AB}{ACTR - AB} \times 100\% \quad (9)$$

where CVK is the cell viability of the cells exposed to the decontaminated solution, AK is the absorbance found for cells exposed to decontaminated solutions, AB is the absorbance of the culture medium, and $ACTR$ is the absorbance of the control cells.

3. Results and Discussion

3.1. Membrane characterization

Electrospun membranes have a great advantage when compared to other type of membranes due their large surface area and the presence of pores³⁰. Figure 1 shows the produced membrane 25 mm diameter and the SEM image of the adsorbent membrane used in the decontamination of the tested solution. The image presents a fibrous membrane. This morphology favors the adsorption process due to the pores among the fibers, which allows the infiltration of the

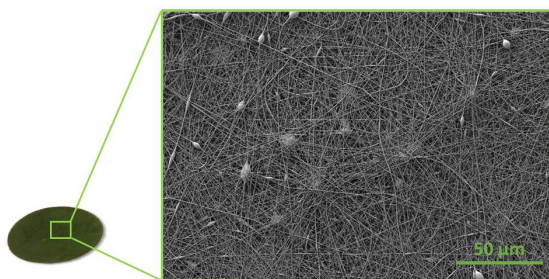


Figure 1. Photograph of the produced nanofibrous membrane 25mm diameter (left) and SEM image of adsorbent membranes morphology (right).

Table 1. Characteristics of the adsorbent membrane.

Thickness (μm)	Contact Angle (θ)	Average Fiber Diameter (nm)	Porosity (%)
234.9 ± 3.7	44.2 ± 2.2	140.7 ± 6.3	76.8 ± 0.1

contaminated solution and, consequently, increases the contact area of metal-membrane^{31,32}. The complementary characterization is presented in Table 1, where the low contact angle provides a high interaction between the adsorbent and the contaminant solution, which is also enhanced by the high porosity obtained (76.8%).

The pH_{PZC} value of the electrospun nanofibrous membrane was 4.18 (Figure 2). Below the pH_{PZC} the surface charges on the adsorbent membrane become positively charged favoring the adsorption of chromate and dichromate ions present in the solution due to the amino group on the membrane surface^{33,34}. The polyaniline amino groups can be protonated at lower pHs and create adsorption sites that allow chromium species to be captured²¹.

The membrane showed a thermal stability property (Figure 3). Both the bulk polymers presented a totally different behavior, the PVDF-HFP has a high thermal stability, with degradation onset at 413 °C and one main degradation peak at 448 °C, similar with the previous literature^{35,36}, which refers to the backbone degradation of PVDF-HFP. Meanwhile, the polyaniline structure has been shown to be less stable with increasing temperature. This polymer presents four thermal events which refers to degradation of doped structure of polyaniline (quinoids and benzenoids units). The adsorbent membrane was also analyzed, showing a similar behavior of PVDF-HFP with only one main peak shifted to 371 °C and, with the degradation onset at 293 °C. Thus, the adsorbent membrane has thermal stability to works from room temperature by 100 °C easily.

3.2. Adsorption results

To investigate the capacity of Cr^{VI} adsorption at low concentrations by the electrospun membrane, batch tests were performed at initial Cr^{VI} concentrations and the percentages of contaminant removed are shown in Figure 4. The removal rate of Cr^{VI} by the membrane decreased as the initial concentration of contaminant increase, this rate decreased from 82.4 to 48.4% when the initial chromium concentration reaches from 0.05 to 5.0 mg/L, respectively.

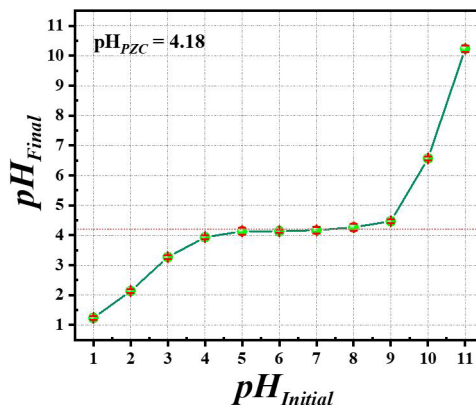


Figure 2. Point of zero charge (pH_{PZC}) of the adsorbent membrane.

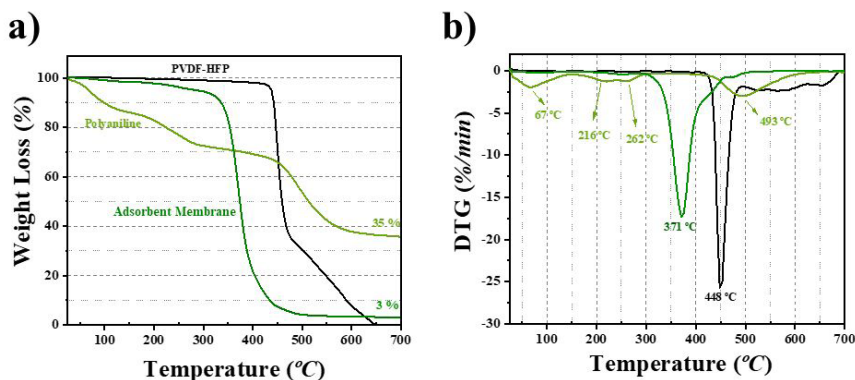


Figure 3. Thermal analysis of bulk PVDF-HFP, Polyaniline and, adsorbent membrane (a) TGA curves and, (b) DTG curves.

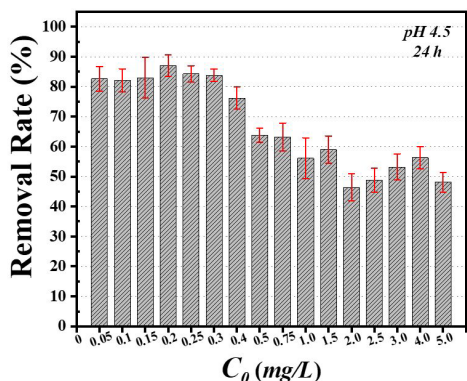


Figure 4. Effect of initial concentration on the percentage of chromium removal (%) at pH 4.5 for 24 h.

According to Wang et al.³⁷, this phenomenon is assigned to the constant amount of surface-active adsorption sites on the membrane. The contact between the metal and the membrane is feasible when the initial chromium concentration is lower due to the small content of chromium.

In order to estimate the adsorption capacity (Q) of the adsorbent, two isotherm models were applied to the mathematical description for the adsorption equilibrium of Cr^{VI} ions on the membrane (Langmuir and Freundlich Models). The results obtained by non-linearized isotherm models are shown in Table 2. The non-linear Langmuir and Freundlich Models are plotted in Figure 5.

The results demonstrated that Freundlich Isotherm Model can better describe the adsorption process with a higher R^2 , which suggests a multilayer adsorption of chromium ions on the membrane, with non-uniform distribution on a heterogeneous surface³⁸. It indicates that polyaniline has different charged regions on the surface or does not fill all the pores onto the membrane causing a heterogeneous coverage. These results were similar to some adsorbent materials used for chromium removal, such as nanochitosan/polyvinyl alcohol/carboxymethyl starch ternary blend³⁹, ionic liquid functionalized cellulose⁴⁰ and, chitosan/nylon 6⁴¹.

Cr^{VI} is highly soluble and mobile in aqueous solutions and generates a significant environmental concern, but it can be reduced to Cr^{III} under some conditions⁴². The use of

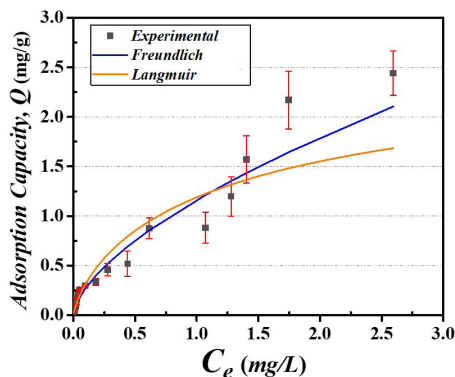


Figure 5. Plot of non-linear Freundlich and Langmuir Isotherm Models for Cr^{VI} adsorption on the nanofibrous membrane at pH 4.5 for 24 h.

Table 2. Constant correlation values for Langmuir and Freundlich adsorption isotherms.

	Langmuir Model		Freundlich Model
R^2	0.89402	R^2	0.95499

polyaniline on the membrane surface allows the adsorption of hexavalent chromium, as described on literature, by two possible steps: (i) reduction of Cr^{VI} to Cr^{III} species by electron donors into the PANi structure and also the possible chemical bond between nitrogen species and Cr^{VI} , with simultaneous oxidation of $-\text{NH}-$ to $=\text{N}-$, and (ii) then the interaction between reduced Cr^{III} and polyaniline^{21,43,44}. This mechanism can corroborate for a possible chemisorption mechanism that is proven by kinetic tests.

The kinetic results, Figure 6, are in accordance with the non-linear form of the kinetic models. The adsorption followed a pseudo second-order reaction, manifested by the better curve fitting observed by the calculated R^2 using OriginPro®, as shown in Table 3. The Cr^{VI} adsorption process by this membrane, at low concentrations of chromium species, is considered as chemisorption process, implying that this process involves valence forces by the sharing or exchange of adsorbent-adsorbate electrons^{37,45}. Nevertheless, this result should be interpreted with some caution once our previous paper²¹ demonstrated that in higher concentrations, over

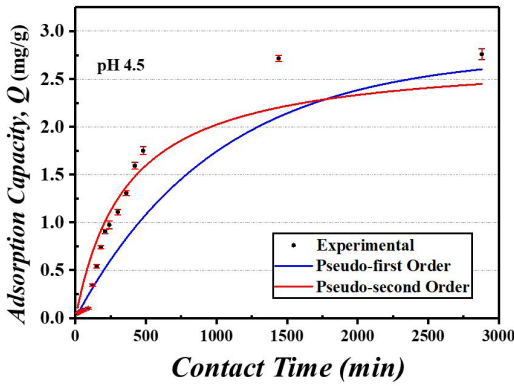


Figure 6. Kinetic curves of Cr^{VI} adsorption by the nanofibrous membrane at pH 4.5 ([Cr^{VI}]=5.0 mg/L).

Table 3. Correlation coefficient values, R^2 , obtained by non-linear form of kinetic model.

	<i>Pseudo-first order</i>		<i>Pseudo-second order</i>
R^2	0.82371	R^2	0.91287

10 mg/L, the kinetic indicates a physisorption process, but for most of the cases there is a combination of chemisorption and physisorption.

Moreover, the initial concentration, the contact time and the pH effect are important factors to describe the adsorption process on the membrane⁴⁶. As shown in Figure 7, a higher percentage of Cr^{VI} removal occurred at pH values between 2 and 6, where is possible to find hydrogen chromate (HCrO₄⁻) and dichromate ions (Cr₂O₇²⁻) as predominant species^{47,48}. This behavior is related to the pH_{PZC} due to fact that at low pH, the protonation of polyaniline enhances Cr^{VI} adsorption.

The thermodynamic parameters, Gibbs free energy change (ΔG°), enthalpy change (ΔH°) and entropy change (ΔS°) were calculated using the experimental data obtained at different temperatures plotted as $\ln K_0$ vs. $1/T$ (Figure 8) and listed in Table 4. The negative values of Gibbs free energy change confirm the feasibility of this process. This result suggests a spontaneous nature of the adsorption at the studied temperatures, and also potentializes the use of this adsorbent in water decontamination^{15,49,50}. The negative enthalpy change indicates that the adsorption reaction was exothermic, thus, the interaction of chromium species and the membrane surface has left energy for the system¹⁵. The decrease in the degree of freedom of the adsorbed chromium was determined by the negative entropy change^{15,51}, which promoted a more ordered interaction to the process.

3.3. MTT assay

Figures 9 and 10 show the effectiveness of the nanofibrous membrane tested in the viability of *D. rerio* fish cells (ZFL). The results of MTT assay (Figure 9) indicate that when ZFL cells were exposed to 2.0-5.0 mg/L of Cr^{VI} and compared to the negative control they showed a decrease in the cell viability. According to the literature, the exposure to chromium may result in cellular toxicity when *in vitro* and *in vivo* systems are employed. Goodale et al.⁵² studied a fish cell line exposed to chromium, and found that the

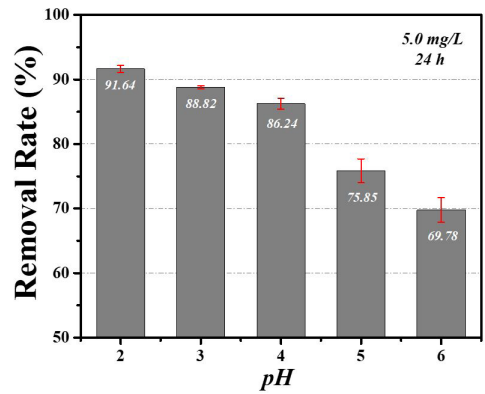


Figure 7. pH effect on the adsorption of Cr^{VI} by the nanofibrous membrane during 24 h ([Cr^{VI}]=5.0 mg/L).

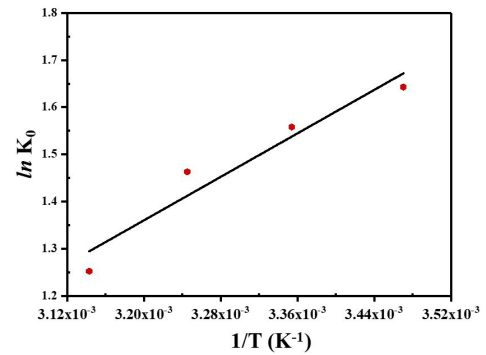


Figure 8. Van't Hoff plot of Cr^{VI} adsorption on the nanofibrous membrane.

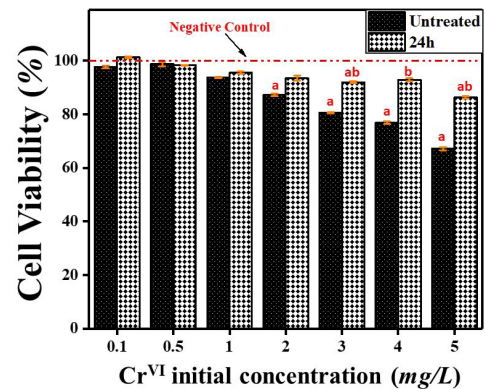
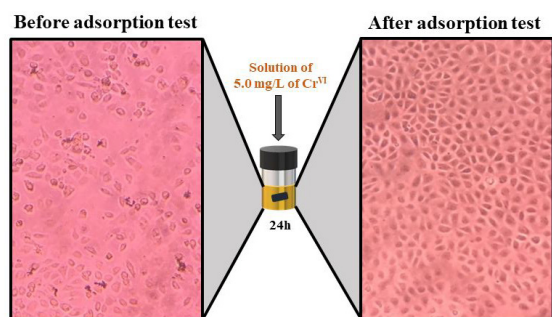


Figure 9. Cell viability (%) of ZFL cells exposed to different concentrations of Cr^{VI} solution, before (Untreated) and after the adsorption test (24h). (*a* and *b* indicate significant difference compared to the negative control and the Untreated solution in the same concentration, respectively).

metal presented a cytotoxicity and genotoxicity activity on these cells. Tan et al.⁵³ evaluated chromium and cadmium cytotoxicity to six different cell lines of fish by MTT assay. After 24 h of exposure, the viability decreased with the increase of the metal concentration. Also, the cell viability percentage of seven cell lines exposed to different chromium

Table 4. Thermodynamic parameters for adsorption of Cr^{VI} on the nanofibrous membrane.

Temperature (K)	K ₀ (m ³ mol ⁻¹)	ΔG° (kJ mol ⁻¹)	ΔH° (kJ mol ⁻¹)	ΔS° (J mol ⁻¹ K ⁻¹)
288.15	5.17	-3.94		
298.15	4.75	-3.86		
308.15	4.32	-3.75	-9.57	-19.32
318.15	3.50	-3.32		

**Figure 10.** Photograph of ZFL cells exposed to 5.0 mg/L of Cr^{VI} solution before (left) and after (right) the adsorbent membrane contact.

concentrations and the toxicity of all the studied lines were reported by Taju et al.⁵⁴. In this paper, the decrease in cells viability of ZFL cells exposed to Cr^{VI} proved to be dosage-dependent, and in the highest concentration (5.0 mg/L), a cell mortality around 32% was verified.

With the increase of the contaminant concentration, the cells viability tended to decrease due to the toxic medium in which the ZFL cells were exposed. However, after 24h in contact with the adsorbent membrane, the free chromium species in the solution were present in lower amount. The highest concentration of these species (5.0 mg/L) provided a higher cell viability of 19.2% for ZFL cells (from 67.1 to 86.3%), as observed in Figure 10.

For the cells exposed to Cr^{VI} 5.0 mg/L, rounded cells, slower cell growth, cell lysis and destroyed cell layer fragments were observed. For the cells exposed to the same concentration (5.0 mg/L) after the adsorption process, the identified morphological changes were milder, as it has caused less damage to the cells.

Therefore, the results of MTT assay indicate that the membrane decreased the chromium concentration in the solution and, consequently, increased the cell viability of the fish cell line tested. As a result, the membrane can be applied to decontamination systems and enable the aquatic life to survive in ecosystems after the adsorption treatment.

4. Conclusion

In the present study, the behavior of low concentration Cr^{VI} adsorption on nanofibrous membrane of coated-polyaniline electrospun PVDF-HFP was investigated. The membrane presented high adsorption capacity simulating an industrial effluent released into the environment. The percentage of removal was over 80% for Cr^{VI} at 0.3 mg/L. In addition, the kinetic and thermodynamic parameters for this process were studied. The time effect showed that the adsorption occurred in pseudo-second order indicating a chemisorption process. The thermodynamic studies demonstrated that the process

was spontaneous and exothermic. Lastly, the cells viability was tested after the decontamination process using the membrane as adsorbent and, the results showed an increase of 19.2% of ZFL cells viability. Therefore, this material can be applied to decontamination systems in order to protect the aquatic ecosystems from Cr^{VI} contaminated effluents.

5. Acknowledgments

The authors would like to thank FAPESP-Brazil (Sao Paulo Research Foundation) [grant number 2015/21261-2, 2016/06288-4 and 2017/03638-7] for the financial support. This study was also financed in part by the Coordenação de Aperfeiçoamento de Pessoal de Nível Superior - Brazil (CAPES) - Finance Code 001. We would also like to thank LabMMEV- FCT/UNESP for the SEM image.

6. References

- Cipullo S, Snapir B, Tardif S, Campo P, Prpich G, Coulon F. Insights into mixed contaminants interactions and its implication for heavy metals and metalloids mobility, bioavailability and risk assessment. *Sci Total Environ.* 2018;645:662-73.
- Kibuye FA, Gall HE, Veith TL, Elkin KR, Elliott HA, Harper JP, et al. Influence of hydrologic and anthropogenic drivers on emerging organic contaminants in drinking water source in the Susquehanna River Basin. *Chemosphere.* 2020;245:125583.
- Galletti C, Dosa M, Russo N, Fino D. Zn²⁺ and Cd²⁺ removal from waste using clinoptilolite as adsorbent. *Environ Sci Pollut Res Int.* 2021;28(19):24355-61. <http://dx.doi.org/10.1007/s11356-020-08483-z>.
- Mahar FK, He L, Wei K, Mehdi M, Zhu M, Gu J, et al. Rapid adsorption of lead ions using porous carbon nanofibers. *Chemosphere.* 2019;225:360-7.
- Liu W, Xu H, Liao Y, Wang Y, Yan N, Qu Z. Co-doped ZnS with large adsorption capacity for recovering Hg⁰ from non-ferrous metal smelting gas as a co-benefit of electrostatic demisters. *Environ Sci Pollut Res Int.* 2020;27:20469-77. <http://dx.doi.org/10.1007/s11356-020-08401-3>.
- Nriagu JO, Nieboer E. Chromium in the natural and human environment. New York: Wiley; 1988.
- Nasir AM, Goh PS, Abdullah MS, Ng BC, Ismail AF. Adsorptive nanocomposite membranes for heavy metal remediation: recent progresses and challenges. *Chemosphere.* 2019;232:96-112.
- Tangahu BV, Sheikh Abdullah SR, Basri H, Idris M, Anuar N, Mukhlisin M. A review on heavy metals (As, Pb, and Hg) uptake by plants through phytoremediation. *Int J Chem Eng.* 2011;2011:939161.
- Masindi V, Muedi KL. Environmental contamination by heavy metals. In: Saleh H, Aglan R, editors. *Heavy metals.* London: IntechOpen; 2018. Chapter 7.
- Engwa GA, Ferdinand PU, Nwalo FN, Unachukwu MN. Mechanism and health effects of heavy metal toxicity in humans. In: Karcioğlu O, Arslan B, editors. *Poisoning in the modern world: new tricks for an old dog?* London: IntechOpen; 2019. Chapter 5.

11. Jaishankar M, Tseten T, Anbalagan N, Mathew BB, Beeregowda KN. Toxicity, mechanism and health effects of some heavy metals. *Interdiscip Toxicol.* 2014;7(2):60-72.
12. Morcillo P, Esteban MA, Cuesta A. Heavy metals produce toxicity, oxidative stress and apoptosis in the marine teleost fish SAF-1 cell line. *Chemosphere.* 2016;144:225-33.
13. Xie B, Shan C, Xu Z, Li X, Zhang X, Chen J, et al. One-step removal of Cr(VI) at alkaline pH by UV/sulfite process: reduction to Cr(III) and in situ Cr(III) precipitation. *Chem Eng J.* 2017;308:791-7.
14. Welch CM, Nekrassova O, Compton RG. Reduction of hexavalent chromium at solid electrodes in acidic media: reaction mechanism and analytical applications. *Talanta.* 2005;65:74-80.
15. Kumar V, Dwivedi SK. Hexavalent chromium reduction ability and bioremediation potential of *Aspergillus flavus* CR500 isolated from electroplating wastewater. *Chemosphere.* 2019;237:124567.
16. Patra DK, Pradhan C, Patra HK. In situ study of growth of lemongrass *Cymbopogon flexuosus* (Nees ex Steud.) W. Watson on varying concentration of chromium (Cr⁶⁺) on potential and phytostabilisation of chromium toxicity. *Chemosphere.* 2018;193:793-9.
17. Qiu B, Xu C, Sun D, Yi H, Guo J, Zhang X, et al. Polyaniline coated ethyl cellulose with improved hexavalent chromium removal. *ACS Sustain Chem& Eng.* 2014;2(8):2070-80.
18. Huang X, Dognani G, Hadi P, Yang M, Job AE, Hsiao BS. Cationic dialdehyde nanocellulose from sugarcane bagasse for efficient chromium (VI) removal. *ACS Sustainable Chem. Eng.* 2020;8:4734-44.
19. Dindar MH, Yaftian MR, Rostamnia S. Potential of functionalized SBA-15 mesoporous materials for decontamination of water solutions from Cr(VI), As(V) and Hg(II) ions. *J Environ Chem Eng.* 2015;3(2):986-95.
20. Dindar MH, Yaftian MR, Hajjhasani M, Rostamnia S. Refinement of contaminated water by Cr(VI), As(V) and Hg(II) using N-donor ligands arranged on SBA-15 platform; batch and fixed-bed column methods. *J Taiwan Inst Chem Eng.* 2016;67:325-37.
21. Dognani G, Hadi P, Ma H, Cabrera FC, Job AE, Agostini DLS, et al. Effective chromium removal from water by polyaniline-coated electrospun adsorbent membrane. *Chem Eng J.* 2019;372:341-51.
22. Adam MR, Hubadillah SK, Esham MIM, Othman MHD, Rahman MA, Ismail AF, et al. Adsorptive membranes for heavy metals removal from water. In: Ismail AF, Rahman MA, Othman MHD, Matsuu T, editors. *Membrane separation principles and applications: from material selection to mechanisms and industrial uses.* 1st ed. Elsevier; 2019. Chapter 12.
23. Anderson SJ, Sposito G. Cesium adsorption method for measuring accessible structural surface charge. *Soil Sci Soc Am J.* 1991;55(6):1569-76.
24. Regalbutto JR, Robles J. The engineering of Pt/carbon catalyst preparation for application on Proton Exchange Fuel Cell Membrane (PEFCM). Chicago: University of Illinois; 2004. p. 1-14.
25. Clesceri LS, Greenberg AE, Eaton AD. Standard methods for the examination of water and wastewater. 20th ed. Maryland, USA: American Public Health Association; 1998.
26. Chen X. Modeling of experimental adsorption isotherm data. *Information.* 2015;6(1):14-22.
27. Moussout H, Ahlafi H, Aazza M, Maghat H. Critical of linear and nonlinear equations of pseudo-first order and pseudo-second order kinetic models. *Karbala Intern J Modern Sci.* 2018;4(2):244-54.
28. Hu X, Wang J, Liu Y, Li X, Zeng G, Bao Z, et al. Adsorption of chromium (VI) by ethylenediamine-modified cross-linked magnetic chitosan resin: isotherm, kinetics and thermodynamics. *J Hazard Mater.* 2011;185(1):306-14.
29. Cavalcante DGS, Silva NDG, Marcarini JC, Mantovani MS, Marin-Morales MA, Martinez CBR. Cytotoxic, biochemical and genotoxic effects of biodiesel produced by different routes on ZFL cell line. *Toxicol In Vitro.* 2014;28(6):1117-25.
30. Dognani G, Cabrera FC, Job AE, Agostini DLS. Morphology of electrospun non-woven membranes of poly(vinylidene fluoride-co-hexafluoropropylene): porous and fibers. *Fibers and Polymers.* 2019;20(3):512-9.
31. Bai L, Jia L, Yan Z, Liu Z, Liu Y. Plasma-etched electrospun nanofiber membrane as adsorbent for dye removal. *Chem Eng Res Des.* 2018;132:445-51.
32. Yuan J, Gao R, Wang Y, Cao W, Yun Y, Dong B, et al. A novel hydrophobic adsorbent of electrospun SiO₂@MUF/PAN nanofibrous membrane and its adsorption behavior oil and organic solvents. *J Mater Sci.* 2018;53(24):16357-70.
33. Bassyouni D, Mohamed M, El-Ashtouky E, El-Latif MA, Zaatout A, Hamad H. Fabrication and characterization of electrospun Fe₃O₄/o-MWCNTs/Polyamide 6 hybrid nanofibrous membrane composite as an efficient and recoverable adsorbent for removal of Pb(II). *Microchem J.* 2019;149:103998.
34. Sahebamee N, Soltanieh M, Mousavi SM, Heydarinasab A. Removal of Cu²⁺, Cd²⁺ and Ni²⁺ ions from aqueous solution using a novel chitosan/polyvinyl alcohol adsorptive membrane. *Carbohydr Polym.* 2019;210:264-73.
35. Liu J, Khanam Z, Muchakayala R, Song S. Fabrication and characterization of Zn-ion conducting solid polymer electrolyte films based on PVDFHFP/Zn(Tf)₂ complex system. *J Mater Sci Mater Electron.* 2020;31(8):6160-73.
36. Ahmad AL, Farooqui UR, Hamid NA. Effect of graphene oxide (GO) on Poly(vinylidene fluoridehexafluoropropylene) (PVDF-HFP) polymer electrolyte membrane. *Polymer.* 2018;142:330-6.
37. Wang XL, Li Y, Huang J, Zhou YZ, Li BL, Liu DB. Efficiency and mechanism of adsorption of low concentration uranium and water by extracellular polymeric substances. *J Environ Radioact.* 2019;197:81-9.
38. Foo KY, Hameed BH. Insights into the modeling of adsorption isotherm systems. *Chem Eng J.* 2010;156(1):2-10.
39. Rajeshwari K, Latha S, Gomathi T, Sangeetha K, Sudha PN. Adsorption of heavy metal Cr (VI) by a ternary biopolymer blend. *Mater Today Proc.* 2018;5:14628-38.
40. Dong Z, Zhao L. Covalent bonded ionic liquid onto cellulose for fast adsorption and efficient separation of Cr(VI): Batch, column and mechanism investigation. *Carbohydr Polym.* 2018;189:190-7.
41. Kummer G, Schonhart C, Fernandes MG, Dotto GL, Missio AL, Bertuol DA, et al. Development of nanofibers composite of chitosan/nylon 6 and tannin/nylon 6 for effective adsorption of Cr(VI). *J Polym Environ.* 2018;26(10):4073-84.
42. Li H, Dong X, Silva EB, Oliveira LM, Chen Y, Ma LQ. Mechanisms of metal sorption by biochars: biochar characteristics and modifications. *Chemosphere.* 2017;178:466-78.
43. Jiang Y, Liu Z, Zeng G, Liu Y, Shao B, Li Z, et al. Polyaniline-based adsorbents for removal of hexavalent chromium from aqueous solution: a mini review. *Environ Sci Pollut Res Int.* 2018;25(7):6158-74.
44. Lei C, Wang C, Chen W, He M, Huang B. Polyaniline@magnetic chitosan nanomaterials for highly efficient simultaneous adsorption and in-situ chemical reduction of hexavalent chromium: removal efficacy and mechanisms. *Sci Total Environ.* 2020;733:139316.
45. Wei L, Li Y, Noguera DR, Zhao N, Song Y, Ding J, et al. Adsorption of Cu²⁺ and Zn²⁺ by extracellular polymeric substances (EPS) in different sludges: effect of EPS fractional polarity on binding mechanism. *J Hazard Mater.* 2017;321:473-83.
46. Duranoğlu D, Trochimczuk AW, Beker U. Kinetic and thermodynamics of hexavalent chromium adsorption onto activated carbon derived from acrylonitrile-divinylbenzene copolymer. *Chem Eng J.* 2012;187:193-202.
47. Kazemi M, Jahanshahi M, Peyravi M. Hexavalent chromium removal by multilayer membrane assisted by photocatalytic

- couple nanoparticle from both permeate and retentate. *J Hazard Mater.* 2018;344:12-22.
48. Ren J, Huang X, Wang N, Lu K, Zhang X, Li W, et al. Preparation of polyaniline-coated polyacrylonitrile fiber mats and their application to Cr(VI) removal. *Synth Met.* 2016;222:255-66.
 49. Souza JVTM, Massocatto CL, Diniz KM, Tarley CRT, Caetano J, Dragunski DC. Adsorption of chromium (III) by waste orange raw and chemically modified. *Semin Ciênc Exatas Tecnol.* 2012;33(1):3-16.
 50. Toledo TV, Bellato CR, Pessoa KD, Fontes MPF. Remoção de Cromo (VI) de soluções aquosas utilizando o compósito magnético calcinado hidrotalcita-óxido de ferro: estudo cinético e de equilíbrio termodinâmico. *Quim Nova.* 2013;36(3):419-25.
 51. Aydın YA, Aksoy ND. Adsorption of chromium on chitosan: optimization, kinetics and thermodynamics. *Chem Eng J.* 2009;151(1-3):188-94.
 52. Goodale BC, Walter R, Pelsue SR, Thompson WD, Wise SS, Winn RN, et al. The cytotoxicity and genotoxicity of hexavalent chromium in medaka (*Oryzias latipes*) cells. *Aquat Toxicol.* 2008;87(1):60-7.
 53. Tan F, Wang M, Wang W, Lu Y. Comparative evaluation of the cytotoxicity sensitivity of six fish cell lines to four heavy metals in vitro. *Toxicol In Vitro.* 2008;22(1):164-70.
 54. Taju G, Abdul Majeed S, Nambi KSN, Sahul Hameed AS. Application of fish cell lines for evaluating the chromium induced cytotoxicity, genotoxicity and oxidative stress. *Chemosphere.* 2017;184:1-12.